Correlation transfer equation for ultrasound-modulated multiply scattered light

Sava Sakadžić and Lihong V. Wang*
Optical Imaging Laboratory, Department of Biomedical Engineering, Texas A&M University, College Station, Texas 77843-3120, USA
(Received 10 April 2006; revised manuscript received 10 August 2006; published 26 September 2006)

In this paper, we develop a temporal correlation transfer equation (CTE) for ultrasound-modulated multiply scattered light. The equation can be used to obtain the time-varying specific intensity of light produced by a nonuniform ultrasound field in optically scattering media that have a heterogeneous distribution of optical parameters. We also develop a Monte Carlo algorithm that can provide the spatial distribution of the optical power spectrum in optically scattering media with focused ultrasound fields, and heterogeneous distributions of optically scattering and absorbing objects. Derivation of the CTE is based on the ladder diagram approximation of the Bethe-Salpeter equation that assumes moderate ultrasound pressures. We expect the CTE to be applicable to a wide spectrum of conditions in the ultrasound-modulated optical tomography of soft biological tissues.

DOI: 10.1103/PhysRevE.74.036618 PACS number(s): 42.25.Dd, 42.90.+m

I. INTRODUCTION

The development of soft biological tissue imaging systems based on ultrasound-modulated multiply scattered light has been a subject of intense research in recent years. The information obtained by exposing the biological tissues to visible and near-infrared radiation can be used for functional imaging and the detection of tissue abnormalities, which make the optical imaging modalities very attractive for medical applications. However, the strong diffusion of light at these wavelengths makes it difficult to obtain good spatial resolution at imaging depths greater than one optical transport mean free path. At present, the application of sophisticated reconstruction algorithms is necessary in order to achieve reasonable spatial resolution in the pure optical imaging modalities, such as diffuse optical tomography, at imaging depths where light is completely diffused [1].

Ultrasound-modulated optical tomography (UOT) is a hybrid technique which combines the advantages of ultrasonic resolution and optical contrast [2,3]. In this technique, focused ultrasound and optical radiation of high temporal coherence are simultaneously applied to soft biological tissue, and the resulting ultrasound-modulated light is then detected. This provides information about the optical properties of the tissue, spatially localized at the interaction region of the ultrasonic and the electromagnetic waves. It is assumed that most of the measured signal comes from the ultrasound focal zone, the position of which can be well controlled due to the low scattering coefficient of ultrasound. Thus, images based on the optical properties of a tissue sample are created by scanning the ultrasound beam.

Due to the very small ratio between the temporal frequencies of the ultrasound and light used in UOT experiments, detection of ultrasound-modulated light belongs to the high-resolution optical spectroscopy domain. Detection has proven to be very challenging because of the uncorrelated optical phases among the speckles that are created by diffused light. Therefore, a great deal of research is currently being directed toward the development of more efficient detection techniques for UOT experiments [3–16].

Simultaneously, progress is being made on the theoretical understanding of the ultrasound modulation of light in optically strongly scattering media. Two mechanisms of modulation are included in the present models. The first mechanism is dynamic light scattering by optical scatterers oscillating in an ultrasound field [4,17], a phenomenon that is largely analogous to dynamic light scattering by scatterers undergoing Brownian motion [18]. The second mechanism accounts for ultrasound-induced changes in the optical index of refraction [19,20]. Both mechanisms have been combined by Wang [20], in a model based on the diffusing-wave spectroscopy (DWS) approach [18,21]. In this model [20], the interaction of a plane ultrasound wave with diffused light is considered in an infinite and homogeneous optically scattering slab, assuming small values of the ultrasound-induced optical phase increments. Subsequently, the equations were extended to account for anisotropic optical scattering [22], Brownian motion [22,23], and strong correlations [24] between the ultrasound-induced optical phase increments. It was shown [24] that the correlations are weak only if $k_a l_{tr} \gg 1$, where l_{tr} is the optical transport mean free path; $k_a = 2\pi/\lambda_a$ is the magnitude of the ultrasound wave vector; and λ_a is the ultrasound wavelength. In the case of anisotropic optical scattering, equations derived for the isotropic case can be applied if l_{tr} is used instead of the optical scattering mean free path l_s [22,24]. In addition, based on a theoretical model, we developed a Monte Carlo algorithm to use for comparison with the theoretical predictions [22,25] as well as for modeling the scattering samples that have optically absorbing objects with cylindrical shapes [26].

Since the existing theoretical model is based on the DWS approach, applications are limited to simple geometries where it is possible to approximate the ultrasound field with a plane ultrasound wave and where the probability density function of the optical path length between the source and detector is analytically known. As a result, only transmission through [20,22,24], and reflection from [23,24], an infinite scattering slab filled with ultrasound, have been analytically studied. In most experiments, however, the optical parameters are heterogeneously distributed and a focused ultra-

*Electronic address: lwang@bme.tamu.edu

 ©2006 The American Physical Society

sound beam is used. Therefore, a more general theoretical model, which can locally treat interactions between ultrasound and light in an optically scattering medium, is needed.

In this paper, based on the ladder diagram approximation of the Bethe-Salpeter equation [27], we have derived a temporal correlation transfer equation (CTE) for ultrasound-modulated multiply scattered light. The work of the many authors who established the link between multiple scattering theory and the radiative transfer equation in the last 60 years was reviewed in several excellent papers [28–33]. Also, several authors have considered the development of the CTE for scatterers moving with a given velocity distribution or undergoing Brownian motion [34–37]. In our case, both the ultrasound-induced movement of the scatterers and the ultrasound-induced change in the optical index of refraction have led to a new form of CTE.

The derivation of the CTE was performed in several steps. In Sec. II, we first develop an expression for the electric field Green's function in the presence of an ultrasound field in a medium free of optical scatterers. Next, we solve the Dyson equation [27] and obtain the value of a mean Green's function in the presence of optical scatterers, which can be used to obtain the ensemble averaged field for a given distribution of optical sources. Finally, in Sec. III, based on the Bethe-Salpeter equation, we write the expression for a mutual coherence function of the electric field and transform it into an integral form of the CTE. Consequently, we derive a differential form of the CTE. In Sec. IV, based on the CTE, we develop a Monte Carlo algorithm. We further calculate the three-dimensional distribution of the power spectrum of the ultrasound-modulated light, produced by 1 MHz focused ultrasound in an optically scattering slab with optical parameters representative of those in soft biological tissues at visible and near infrared wavelengths.

II. DEVELOPMENT OF THE MEAN GREEN'S FUNCTION

We start by presenting an approximate expression for the Green's function of the electric field component in a medium free from optical scatterers in the presence of an ultrasound field. We assume that the dielectric constant of the medium (ϵ) experiences small perturbations due to the ultrasound field and that it is well approximated with $\epsilon=\epsilon_0[1+2\eta P(\mathbf{r},t)/(\rho v_a^2)]$, where ϵ_0 is the dielectric constant of the unperturbed medium; $P(\mathbf{r},t)$ is the ultrasound pressure; ρ is the mass density of the medium; v_a is the ultrasound speed; and η is the elasto-optical coefficient (in water at standard conditions $v_a \approx 1480$ ms^{-1}; and $\eta \approx 0.32$). Consequently, we locally approximate the optical index of refraction with $n(\mathbf{r},t)=n_0[1+\eta P(\mathbf{r},t)/(\rho v_a^2)]$, where $n_0=\sqrt{\epsilon_0}$. Let $F(\mathbf{r})$ be the spatial distribution of a monochromatic light source having angular frequency ω_0 and wave-vector magnitude $k_0=\omega_0/c_0$, where c_0 is the speed of light in vacuum. To simplify the derivations, we neglect the optical polarization effects and consider only one component $\tilde{E}(\mathbf{r},t)$ of the electric field. The time retardation is also neglected, since the time during which the light propagates through the sample is a small fraction of the ultrasound period. Due to the large ratio between the optical and ultrasound temporal frequencies, we approximate the quasi-monochromatic electric field in the medium as $\tilde{E}(\mathbf{r},t)=E(\mathbf{r},t)\exp(-i\omega_0 t)$, where $E(\mathbf{r},t)$ is a slowly changing function of time that satisfies the following equation:

$$\left[\nabla^2 + k_0^2 n_0^2\left(1 + 2\frac{\eta P(\mathbf{r},t)}{\rho v_a^2}\right)\right]E(\mathbf{r},t) = F(\mathbf{r}), \tag{1}$$

where $2\eta P(\mathbf{r},t)/(\rho v_a^2) \ll 1$.

For a point source at position $\mathbf{r}_0$, $F(\mathbf{r})=\delta(\mathbf{r}-\mathbf{r}_0)$, where $\delta(\ )$ is the Dirac delta function, and the solution of Eq. (1) is the Green's function $G_a(\mathbf{r},\mathbf{r}_0,t)$. We present $G_a(\mathbf{r},\mathbf{r}_0,t)$ as

$$G_a(\mathbf{r},\mathbf{r}_0,t) = \frac{\exp\{ik_0 n_0|\mathbf{r}-\mathbf{r}_0|[1+\xi(\mathbf{r},\mathbf{r}_0,t)]\}}{-4\pi|\mathbf{r}-\mathbf{r}_0|}, \tag{2}$$

where the small fractional phase perturbation $\xi(\mathbf{r},\mathbf{r}_0,t)$ is the slowly varying function of $P(\mathbf{r},t)$ and where $k_0 n_0|\mathbf{r}-\mathbf{r}_0|\,\xi(\mathbf{r},\mathbf{r}_0,t)$ vanishes whenever $\mathbf{r}\to\mathbf{r}_0$ or $2\eta P(\mathbf{r},t)/(\rho v_a^2)\to 0$. We consider moderate ultrasound pressures and distances $\mathbf{r}$ not far from the source position $\mathbf{r}_0$ such that $k_0 n_0|\mathbf{r}-\mathbf{r}_0|\,\xi(\mathbf{r},\mathbf{r}_0,t) \ll 1$, and we approximate $\xi(\mathbf{r},\mathbf{r}_0,t)$ with an integral over the optical path increments along the line between $\mathbf{r}_0$ and $\mathbf{r}$ as

$$\xi(\mathbf{r},\mathbf{r}_0,t) = \frac{\eta}{\rho v_a^2|\mathbf{r}-\mathbf{r}_0|}\int_{\mathbf{r}_0}^{\mathbf{r}} P(\mathbf{r}',t)dr'. \tag{3}$$

By performing the integration in Eq. (3) along the straight line which connects $\mathbf{r}_0$ and $\mathbf{r}$, we assume that the ultrasound-induced refraction of the optical waves is negligible for the interaction length $|\mathbf{r}-\mathbf{r}_0|$.

We then consider a medium with discrete and uncorrelated optical scatterers. We assume independent optical scattering and an optical wavelength λ_0 that is much smaller than l_s (weak scattering approximation). We also assume that a monochromatic ultrasound field, in an optically scattering medium representative of soft biological tissue, is uniform on scales that are comparable with l_{tr}, and we locally approximate the ultrasound pressure with $P(\mathbf{r},t)=P_0\cos(\omega_a t - \mathbf{k}_a\cdot\mathbf{r}+\phi)$, where $\mathbf{k}_a=k_a\hat{\mathbf{\Omega}}_a$ is the ultrasound wave vector and P_0, ω_a, ϕ, and $\hat{\mathbf{\Omega}}_a$ are the pressure amplitude, angular frequency, local initial phase, and propagation direction unit vector of the ultrasound, respectively ($|\hat{\mathbf{\Omega}}_a|=1$). This allows us to write an explicit expression for the fractional phase perturbation $\xi(\mathbf{r},\mathbf{r}_0,t)$ as

$$\xi(\mathbf{r},\mathbf{r}_0,t) = \frac{1}{2}M\cos\left(\omega_a t - \mathbf{k}_a\cdot\frac{\mathbf{r}+\mathbf{r}_0}{2}+\phi\right)\mathrm{sinc}\left(\mathbf{k}_a\cdot\frac{\mathbf{r}-\mathbf{r}_0}{2}\right), \tag{4}$$

where $\mathrm{sinc}(x)=\sin(x)/x$, and $M=2\eta P_0/(\rho v_a^2)$.

The accuracy of Eq. (2) with $\xi(\mathbf{r},\mathbf{r}_0,t)$ given by Eq. (4) is worse for large values of $|\mathbf{r}-\mathbf{r}_0|$. For further derivations, Eq. (2) is required to be approximately valid for $|\mathbf{r}-\mathbf{r}_0|$ on the order of a few l_{tr}. This requirement is satisfied in soft biological tissues at visible and near-infrared optical wavelengths ($l_{tr}\approx 1$ mm), for moderate ultrasound pressures

($P_0 \leqslant 10^5$ Pa) and in the medical ultrasound frequency range [24].

The scattering cross section σ_s is related to the optical scattering amplitude $f(\hat{\mathbf{\Omega}}_{\rm sc},\hat{\mathbf{\Omega}}_{\rm inc})$ as $\sigma_s=\int_{4\pi}|f(\hat{\mathbf{\Omega}}_{\rm sc},\hat{\mathbf{\Omega}}_{\rm inc})|^2 \times d\Omega_{\rm sc}$, where $\hat{\mathbf{\Omega}}_{\rm inc}$ and $\hat{\mathbf{\Omega}}_{\rm sc}$ are the directions of the incident and scattered waves, respectively, and we assume that the scattering potential is spherically symmetric such that $f(\hat{\mathbf{\Omega}}_{\rm sc},\hat{\mathbf{\Omega}}_{\rm inc})$ is a function of $\hat{\mathbf{\Omega}}_{\rm sc}\cdot\hat{\mathbf{\Omega}}_{\rm inc}$ only. The scattering phase function $p(\hat{\mathbf{\Omega}}_{\rm sc},\hat{\mathbf{\Omega}}_{\rm inc})$ is defined as $p(\hat{\mathbf{\Omega}}_{\rm sc},\hat{\mathbf{\Omega}}_{\rm inc}) =\sigma_s^{-1}|f(\hat{\mathbf{\Omega}}_{\rm sc},\hat{\mathbf{\Omega}}_{\rm inc})|^2$, and it satisfies $\int_{4\pi}p(\hat{\mathbf{\Omega}}_{\rm sc},\hat{\mathbf{\Omega}}_{\rm inc})d\Omega_{\rm sc}=1$. In addition, from the optical theorem, we have $\sigma_s+\sigma_a =4\pi\,{\rm Im}[f(\hat{\mathbf{\Omega}}_{\rm inc},\hat{\mathbf{\Omega}}_{\rm inc})]/(k_0n_0)$, where σ_a is the optical absorption cross section, and Im[ ] is an imaginary part. If ρ_s is the density of optical scatterers, then the optical extinction, scattering and absorption coefficients are defined as $\mu_t=\mu_s +\mu_a$, $\mu_s=\sigma_s\rho_s$, and $\mu_a=\sigma_a\rho_s$, respectively.

We assume sufficiently small optical scatterers and consider only the far field approximations of the scattered fields. The far field approximation of field $E_s(\mathbf{r},t)$ produced by the scattering of the plane wave $\exp(ik_0n_0\hat{\mathbf{\Omega}}_{\rm inc}\cdot\mathbf{r})$ from the single optical scatterer at $\mathbf{r}_s$ is given by

$$E_s(\mathbf{r},t) = -4\pi G_a(\mathbf{r},\mathbf{r}_s,t)f(\hat{\mathbf{\Omega}}_{\rm sc},\hat{\mathbf{\Omega}}_{\rm inc})\exp[ik_0n_0\mathbf{e}_s(t)\cdot(\hat{\mathbf{\Omega}}_{\rm inc} - \hat{\mathbf{\Omega}}_{\rm sc})]\exp(ik_0n_0\hat{\mathbf{\Omega}}_{\rm inc}\cdot\mathbf{r}_s), \quad (5)$$

where $\hat{\mathbf{\Omega}}_{\rm sc}=(\mathbf{r}-\mathbf{r}_s)/|\mathbf{r}-\mathbf{r}_s|$ and the refraction of the optical waves due to the ultrasound field is neglected. The first exponential factor on the right-hand side of Eq. (5) accounts for the Doppler shift caused by the ultrasound-induced movement of the scatterer. The position of the scatterer at moment t is $\mathbf{r}_s+\mathbf{e}_s(t)$, where $\mathbf{r}_s$ is the resting position and $\mathbf{e}_s(t)$ is the small ultrasound-induced displacement given by $\mathbf{e}_s(t)=\hat{\mathbf{\Omega}}_aP_0S_a(k_a\rho v_a^2)^{-1}\sin(\omega_at-\mathbf{k}_a\cdot\mathbf{r}_s-\phi_a+\phi)$. In general, S_a and ϕ_a represent the deviations of the amplitude and the phase of the scatterer displacement from the movement of the surrounding fluid [24,38]. However, we expect that an endogenous optical scatterer in soft biological tissue closely follows the ultrasound-induced "background" tissue vibrations, i.e., $S_a\approx 1$ and $\phi_a\approx 0$.

When multiple scattering is considered, the mean Green's function $G_s(\mathbf{r}_b,\mathbf{r}_a,t)$ provides the ensemble averaged value of the electric field (referred to also as a mean or coherent field) at $\mathbf{r}_b$ emitted from a point source at $\mathbf{r}_a$. We obtain $G_s(\mathbf{r}_b,\mathbf{r}_a,t)$ by solving the Dyson equation [27,34,35], whose far-field expression in the Bourret approximation is given by

$$G_s(\mathbf{r}_b,\mathbf{r}_a,t) = G_a(\mathbf{r}_b,\mathbf{r}_a,t) - 4\pi\rho_s\int G_a(\mathbf{r}_b,\mathbf{r}_s,t)f(\hat{\mathbf{\Omega}}_{sb},\hat{\mathbf{\Omega}}_{as}) \times\exp[ik_0n_0\mathbf{e}_s(t)\cdot(\hat{\mathbf{\Omega}}_{as}-\hat{\mathbf{\Omega}}_{sb})]G_s(\mathbf{r}_s,\mathbf{r}_a,t)d\mathbf{r}_s. \quad (6)$$

In Eq. (6), $\hat{\mathbf{\Omega}}_{as}$ and $\hat{\mathbf{\Omega}}_{sb}$ are unity vectors in directions $\mathbf{r}_s-\mathbf{r}_a$ and $\mathbf{r}_b-\mathbf{r}_s$, respectively, and the refraction of the mean optical field that is due to the ultrasound is neglected.

By applying the method of stationary phase to Eq. (6), we obtain the following solution (see the Appendix):

$$G_s(\mathbf{r}_b,\mathbf{r}_a,t) = \frac{\exp[iK(\mathbf{r}_b,\mathbf{r}_a,t)|\mathbf{r}_b-\mathbf{r}_a|]}{-4\pi|\mathbf{r}_b-\mathbf{r}_a|}, \quad (7)$$

where

$$K(\mathbf{r}_b,\mathbf{r}_a,t) = k_0n_0[1+\xi(\mathbf{r}_b,\mathbf{r}_a,t)] + 2\pi\rho_s f(\hat{\mathbf{\Omega}},\hat{\mathbf{\Omega}})/(k_0n_0)$$

. The difference between the mean Green's function $G_s(\mathbf{r}_b,\mathbf{r}_a,t)$ given by Eq. (7) and the free-space Green's function $G(\mathbf{r}_b,\mathbf{r}_a,t)=\exp(ik_0n_0|\mathbf{r}_b-\mathbf{r}_a|)/(-4\pi|\mathbf{r}_b-\mathbf{r}_a|)$ is in the form of the propagation constant $K(\mathbf{r}_b,\mathbf{r}_a,t)$. The term $\xi(\mathbf{r}_b,\mathbf{r}_a,t)$ is related to the accumulated optical phase from $\mathbf{r}_a$ to $\mathbf{r}_b$, due to ultrasound-induced changes in the optical index of refraction. The term $2\pi\rho_sf(\hat{\mathbf{\Omega}},\hat{\mathbf{\Omega}})/(k_0n_0)$ accounts for the multiple wave scattering from $\mathbf{r}_a$ to $\mathbf{r}_b$, and its real and imaginary parts are related to the reduction of the propagation speed and the attenuation of the mean field, respectively. Also, in the absence of optical scatterers, the term $2\pi\rho_sf(\hat{\mathbf{\Omega}},\hat{\mathbf{\Omega}})/(k_0n_0)$ vanishes, and $G_s(\mathbf{r}_b,\mathbf{r}_a,t)$ reduces to $G_a(\mathbf{r}_b,\mathbf{r}_a,t)$.

III. DEVELOPMENT OF THE CTE

The mutual coherence function of the electric field component is given by $\Gamma(\mathbf{r}_a,\mathbf{r}_b,t,\tau)=\langle E(\mathbf{r}_a,t)E^*(\mathbf{r}_b,t+\tau)\rangle$, where $\mathbf{r}_a$ and $\mathbf{r}_b$ are two closely spaced points relative to the mean free path l_t, and $\langle\,\rangle$ represents ensemble averaging. We assume a quasiuniform $\Gamma(\mathbf{r}_a,\mathbf{r}_b,t,\tau)$, which varies more slowly in respect to the center of gravity coordinate $\mathbf{r}_c=(\mathbf{r}_a+\mathbf{r}_b)/2$ than in respect to the difference coordinate $\mathbf{r}_d=\mathbf{r}_a-\mathbf{r}_b$ ($|\partial_{\mathbf{r}_c}\Gamma|\ll|\partial_{\mathbf{r}_d}\Gamma|$). Under the weak-scattering approximation, $\Gamma(\mathbf{r}_a,\mathbf{r}_b,t,\tau)$ satisfies the ladder approximation of the Bethe-Salpeter equation [27,34,35,37] for moving scatterers

$$\Gamma(\mathbf{r}_a,\mathbf{r}_b,t,\tau) = \Gamma_0(\mathbf{r}_a,\mathbf{r}_b,t,\tau) + \int\int v_{s'}^a(t)v_{s''}^{b*}(t+\tau) \times\Gamma(\mathbf{r}_{s'},\mathbf{r}_{s''},t,\tau)\rho(\mathbf{r}_{s'},t;\mathbf{r}_{s''},t+\tau)d\mathbf{r}_{s'}d\mathbf{r}_{s''}, \quad (8)$$

where $\Gamma_0(\mathbf{r}_a,\mathbf{r}_b,t,\tau)=\langle E(\mathbf{r}_a,t)\rangle\langle E^*(\mathbf{r}_b,t+\tau)\rangle$ is the mutual coherence function of the coherent (unscattered) field, and $\mathbf{r}_{s'}$ and $\mathbf{r}_{s''}$ are the positions of the same scatterer at time moments t and $t+\tau$, respectively (Fig. 1). The function $\rho(\mathbf{r}_{s'},t;\mathbf{r}_{s''},t+\tau)$ is the probability density of finding the same scatterer s at position $\mathbf{r}_{s'}$ and time t, and at position $\mathbf{r}_{s''}$ and time $t+\tau$. By assuming the far field approximation of the operators $v_{s'}^a(t)$ and $v_{s''}^{b\,*}(t+\tau)$, the factor $v_{s'}^a(t)v_{s''}^{b\,*}(t+\tau)\Gamma(\mathbf{r}_{s'},\mathbf{r}_{s''},t,\tau)$ in Eq. (8) can be written as an integral over all the spectral components of $\Gamma(\mathbf{r}_{s'},\mathbf{r}_{s''},t,\tau)$. The spectral density $\tilde{\Gamma}(\mathbf{r}_{cs},\mathbf{q}',t,\tau)$ of $\Gamma(\mathbf{r}_{s'},\mathbf{r}_{s''},t,\tau)$ is defined as the spatial Fourier transform with respect to the difference variable $\mathbf{r}_{ds}=\mathbf{r}_{s'}-\mathbf{r}_{s''}$,

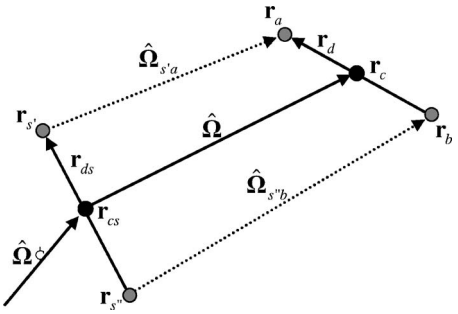

FIG. 1. Coordinates of the moving scatterer and the detection points in the center of gravity coordinate systems.

$$\tilde{\Gamma}(\mathbf{r}_{cs},\mathbf{q}',t,\tau)=(2\pi)^{-3}\int\Gamma(\mathbf{r}_{cs},\mathbf{r}_{ds},t,\tau)\exp(-i\mathbf{q}'\cdot\mathbf{r}_{ds})d\mathbf{r}_{ds}, \tag{9}$$

where $\mathbf{r}_{cs}=(\mathbf{r}_{s'}+\mathbf{r}_{s''})/2$. The formal expressions of the operators $v^a_{s'}(t)$ and $v^{b*}_{s''}(t+\tau)$ in the far-field approximation are given by $V^a_{s'}(t,\hat{\mathbf{\Omega}}')=-4\pi G_s(\mathbf{r}_a,\mathbf{r}_{s'},t)f(\hat{\mathbf{\Omega}}_{s'a},\hat{\mathbf{\Omega}}')$ and $V^{b*}_{s''}(t+\tau,\hat{\mathbf{\Omega}}')=-4\pi G^*_s(\mathbf{r}_b,\mathbf{r}_{s''},t+\tau)f^*(\hat{\mathbf{\Omega}}_{s''b},\hat{\mathbf{\Omega}}')$, respectively, where $\hat{\mathbf{\Omega}}'=\mathbf{q}'/|\mathbf{q}'|$. Finally, the factor $v^a_{s'}(t)v^{b*}_{s''}(t+\tau)\Gamma(\mathbf{r}_{s'},\mathbf{r}_{s''},t,\tau)$ in the integral in Eq. (8) can be written as

$$\begin{aligned}v^a_{s'}(t)v^{b*}_{s''}(t+\tau)\Gamma(\mathbf{r}_{s'},\mathbf{r}_{s''},t,\tau)&\\ \equiv\int V^a_{s'}(t,\hat{\mathbf{\Omega}}')V^{b*}_{s''}(t+\tau,\hat{\mathbf{\Omega}}')\tilde{\Gamma}(\mathbf{r}_{cs},\mathbf{q}',t,\tau)&\\ \times\exp(i\mathbf{q}'\cdot\mathbf{r}_{ds})d\mathbf{q}',&\end{aligned} \tag{10}$$

where

$$\begin{aligned}V^a_{s'}(t,\hat{\mathbf{\Omega}}')V^{b*}_{s''}(t+\tau,\hat{\mathbf{\Omega}}')&\\ =\frac{f(\hat{\mathbf{\Omega}}_{s'a},\hat{\mathbf{\Omega}}')f^*(\hat{\mathbf{\Omega}}_{s''b},\hat{\mathbf{\Omega}}')}{|\mathbf{r}_a-\mathbf{r}_{s'}||\mathbf{r}_b-\mathbf{r}_{s''}|}\exp[iK(\mathbf{r}_a,\mathbf{r}_{s'},t)|\mathbf{r}_a-\mathbf{r}_{s'}|]&\\ \times\exp[-iK^*(\mathbf{r}_b,\mathbf{r}_{s''},t+\tau)|\mathbf{r}_b-\mathbf{r}_{s''}|].&\end{aligned} \tag{11}$$

To simplify the expression on the right-hand side of Eq. (11), we use previously defined vectors in the center-of-gravity coordinate systems $\mathbf{r}_c=(\mathbf{r}_a+\mathbf{r}_b)/2$, $\mathbf{r}_d=\mathbf{r}_a-\mathbf{r}_b$, $\mathbf{r}_{cs}=(\mathbf{r}_{s'}+\mathbf{r}_{s''})/2$, $\mathbf{r}_{ds}=\mathbf{r}_{s'}-\mathbf{r}_{s''}$, and we also define $\hat{\mathbf{\Omega}}=(\mathbf{r}_c-\mathbf{r}_{cs})/|\mathbf{r}_c-\mathbf{r}_{cs}|$. Since $|\mathbf{r}_d|\ll|\mathbf{r}_c-\mathbf{r}_{cs}|$ and $|\mathbf{r}_{ds}|\ll|\mathbf{r}_c-\mathbf{r}_{cs}|$, we assume $f(\hat{\mathbf{\Omega}}_{s'a},\hat{\mathbf{\Omega}}')\approx f(\hat{\mathbf{\Omega}},\hat{\mathbf{\Omega}}')$, $f(\hat{\mathbf{\Omega}}_{s''b},\hat{\mathbf{\Omega}}')\approx f(\hat{\mathbf{\Omega}},\hat{\mathbf{\Omega}}')$, and

$$\begin{aligned}|\mathbf{r}_a-\mathbf{r}_{s'}|&\approx|\mathbf{r}_c-\mathbf{r}_{cs}|+(\mathbf{r}_d-\mathbf{r}_{ds})\cdot\hat{\mathbf{\Omega}}/2,\\ |\mathbf{r}_b-\mathbf{r}_{s''}|&\approx|\mathbf{r}_c-\mathbf{r}_{cs}|-(\mathbf{r}_d-\mathbf{r}_{ds})\cdot\hat{\mathbf{\Omega}}/2,\\ (|\mathbf{r}_a-\mathbf{r}_{s'}||\mathbf{r}_b-\mathbf{r}_{s''}|)^{-1}&\approx|\mathbf{r}_c-\mathbf{r}_{cs}|^{-2}.\end{aligned} \tag{12}$$

Equation (11) can be now presented as

$$\begin{aligned}V^a_{s'}(t,\hat{\mathbf{\Omega}}')V^{b*}_{s''}(t+\tau,\hat{\mathbf{\Omega}}')&\\ =\sigma_s p(\hat{\mathbf{\Omega}},\hat{\mathbf{\Omega}}')|\mathbf{r}_c-\mathbf{r}_{cs}|^{-2}\exp[iK_r(\mathbf{r}_d-\mathbf{r}_{ds})\cdot\hat{\mathbf{\Omega}}&\\ -\mu_t|\mathbf{r}_c-\mathbf{r}_{cs}|]\exp[i\Psi_n(\mathbf{r}_a,\mathbf{r}_b,\mathbf{r}_{s'},\mathbf{r}_{s''},t,\tau)],&\end{aligned} \tag{13}$$

where $K_r=n_0k_0+4\pi\mathrm{Re}[f(\hat{\mathbf{\Omega}},\hat{\mathbf{\Omega}})]\rho_s/(2k_0n_0)$, and Re[ ] is the real part. $\Psi_n(\mathbf{r}_a,\mathbf{r}_b,\mathbf{r}_{s'},\mathbf{r}_{s''},t,\tau)$ is the difference between the ultrasound-induced phase increments given by

$$\begin{aligned}\Psi_n(\mathbf{r}_a,\mathbf{r}_b,\mathbf{r}_{s'},\mathbf{r}_{s''},t,\tau)=k_0n_0|\mathbf{r}_a-\mathbf{r}_{s'}|\xi(\mathbf{r}_a,\mathbf{r}_{s'},t)&\\ -k_0n_0|\mathbf{r}_b-\mathbf{r}_{s''}|\xi(\mathbf{r}_b,\mathbf{r}_{s''},t+\tau).&\end{aligned} \tag{14}$$

By using the relations in Eq. (12), the expression in Eq. (14) is approximated as $\Psi_n(\mathbf{r}_a,\mathbf{r}_b,\mathbf{r}_{s'},\mathbf{r}_{s''},t,\tau)\approx\Psi_n(\mathbf{r}_c,\mathbf{r}_{cs},t,\tau)$, where

$$\begin{aligned}\Psi_n(\mathbf{r}_c,\mathbf{r}_{cs},t,\tau)=\frac{2\Lambda_n k_a}{\mathbf{k}_a\cdot\hat{\mathbf{\Omega}}}\sin\left(\omega_a\frac{\tau}{2}\right)\sin\left[\omega_a\left(t+\frac{\tau}{2}\right)\right.&\\ \left.-\mathbf{k}_a\cdot\frac{\mathbf{r}_c+\mathbf{r}_{cs}}{2}+\phi\right]\sin\left(\mathbf{k}_a\cdot\frac{\mathbf{r}_c-\mathbf{r}_{cs}}{2}\right).&\end{aligned} \tag{15}$$

In Eq. (15), $\Lambda_n=2k_0n_0\eta P_0/(k_a\rho v_a^2)$.

We express the positions $\mathbf{r}_{s'}$ and $\mathbf{r}_{s''}$ of the scatterer at the time moments t and $t+\tau$ as $\mathbf{r}_{s'}=\mathbf{r}_s+\mathbf{e}_s(t)$ and $\mathbf{r}_{s''}=\mathbf{r}_s+\mathbf{e}_s(t+\tau)$, respectively. The probability density function $\rho(\mathbf{r}_{s'},t;\mathbf{r}_{s''},t+\tau)$ in Eq. (8) is given by

$$\rho(\mathbf{r}_{s'},t;\mathbf{r}_{s''},t+\tau)=\rho_s\delta(\mathbf{r}_{ds}-\Delta\mathbf{e}(\mathbf{r}_s,t,\tau)), \tag{16}$$

where $\Delta\mathbf{e}(\mathbf{r}_s,t,\tau)=\mathbf{e}_s(t)-\mathbf{e}_s(t+\tau)$. By replacing the integration over positions $\mathbf{r}_{s'}$ and $\mathbf{r}_{s''}$ with an integration over $\mathbf{r}_{ds}$ and $\mathbf{r}_{cs}$, Eq. (8) becomes

$$\begin{aligned}\Gamma(\mathbf{r}_c,\mathbf{r}_d,t,\tau)=\Gamma_0(\mathbf{r}_c,\mathbf{r}_d,t,\tau)+\int\mu_s p(\hat{\mathbf{\Omega}},\hat{\mathbf{\Omega}}')&\\ \times\exp[iK_r(\mathbf{r}_d-\mathbf{r}_{ds})\cdot\hat{\mathbf{\Omega}}]\exp[i\Psi_n(\mathbf{r}_c,\mathbf{r}_{cs},t,\tau)]&\\ \times\exp(-\mu_t|\mathbf{r}_c-\mathbf{r}_{cs}|)\tilde{\Gamma}(\mathbf{r}_{cs},\mathbf{q}',t,\tau)\exp(i\mathbf{q}'\cdot\mathbf{r}_{ds})&\\ \times\delta(\mathbf{r}_{ds}-\Delta\mathbf{e}(\mathbf{r}_s,t,\tau))d\mathbf{r}_{ds}d|\mathbf{r}_c-\mathbf{r}_{cs}|d\Omega d\mathbf{q}',&\end{aligned} \tag{17}$$

where we used $d\mathbf{r}_{cs}=|\mathbf{r}_c-\mathbf{r}_{cs}|^2d|\mathbf{r}_c-\mathbf{r}_{cs}|d\Omega$. After performing an additional integration over $\mathbf{r}_{ds}$, we have

$$\begin{aligned}\Gamma(\mathbf{r}_c,\mathbf{r}_d,t,\tau)=\Gamma_0(\mathbf{r}_c,\mathbf{r}_d,t,\tau)+\int\mu_s p(\hat{\mathbf{\Omega}},\hat{\mathbf{\Omega}}')&\\ \times\exp(iK_r\mathbf{r}_d\cdot\hat{\mathbf{\Omega}})\exp(-\mu_t|\mathbf{r}_c-\mathbf{r}_{cs}|)&\\ \times\exp[i(\mathbf{q}'-K_r\hat{\mathbf{\Omega}})\cdot\Delta\mathbf{e}(\mathbf{r}_s,t,\tau)]&\\ \times\exp[i\Psi_n(\mathbf{r}_c,\mathbf{r}_{cs},t,\tau)]\tilde{\Gamma}(\mathbf{r}_{cs},\mathbf{q}',t,\tau)&\\ \times d|\mathbf{r}_c-\mathbf{r}_{cs}|d\Omega d\mathbf{q}',&\end{aligned} \tag{18}$$

where $\exp(-\mu_t|\mathbf{r}_c-\mathbf{r}_{cs}|)$ accounts for the attenuation of the field, and the exponential factors that contain $\Delta\mathbf{e}(\,)$ and $\Psi_n(\,)$

are due to the ultrasound-induced optical phase increments.

Equation (18) can be further simplified by realizing that for quasi-monochromatic light, the spectral density $\tilde{\Gamma}(\mathbf{r}_{cs},\mathbf{q}',t,\tau)$ of the quasiuniform mutual coherence function is approximately concentrated on a spherical shell with radius $|\mathbf{q}'|=K_r$ [28,31,32,39,40]. We relate then the time-varying specific intensity $I(\mathbf{r}_{cs},\hat{\mathbf{\Omega}}',t,\tau)$ to the spectral density $\tilde{\Gamma}(\mathbf{r}_{cs},\mathbf{q}',t,\tau)$ by the following approximation [28,29,31,32,37,39,40]:

$$\tilde{\Gamma}(\mathbf{r}_{cs},\mathbf{q}',t,\tau) \approx \delta(|\mathbf{q}'|-K_r)I(\mathbf{r}_{cs},\hat{\mathbf{\Omega}}',t,\tau)/K_r^2. \tag{19}$$

For $\Gamma(\mathbf{r}_c,\mathbf{r}_d,t,\tau)$ and $\Gamma_0(\mathbf{r}_c,\mathbf{r}_d,t,\tau)$, we write the expressions similar to Eqs. (9) and (19) and combine them to obtain the following relations:

$$\Gamma(\mathbf{r}_c,\mathbf{r}_d,t,\tau) = \int I(\mathbf{r}_c,\hat{\mathbf{\Omega}},t,\tau)\exp(iK_r\hat{\mathbf{\Omega}}\cdot\mathbf{r}_d)d\Omega, \tag{20a}$$

$$\Gamma_0(\mathbf{r}_c,\mathbf{r}_d,t,\tau) = \int I_0(\mathbf{r}_c,\hat{\mathbf{\Omega}},t,\tau)\exp(iK_r\hat{\mathbf{\Omega}}\cdot\mathbf{r}_d)d\Omega, \tag{20b}$$

where the time-varying specific intensity is presented as an angular spectrum of the mutual coherence function. From Eq. (20a), we note that the temporal field correlation function $\Gamma(\mathbf{r}_c,0,t,\tau)$ is given by $\int I(\mathbf{r}_c,\hat{\mathbf{\Omega}},t,\tau)d\Omega$. Therefore, the optical power spectrum density of the ultrasound modulated light received in some solid angle Ω_0 can be obtained by the temporal Fourier transform of $I_{\Omega_0}(\mathbf{r}_c,\tau)=\int_{\Omega_0} I(\mathbf{r}_c,\hat{\mathbf{\Omega}},\tau)d\Omega$, where $I(\mathbf{r}_c,\hat{\mathbf{\Omega}},\tau)$ is obtained by averaging the time-varying specific intensity over an ultrasound period as [41]

$$I(\mathbf{r}_c,\hat{\mathbf{\Omega}},\tau) = \frac{\omega_a}{2\pi}\int_0^{2\pi/\omega_a} I(\mathbf{r}_c,\hat{\mathbf{\Omega}},t,\tau)dt. \tag{21}$$

Finally, the integral form of the CTE is obtained by substituting Eqs. (20a), (20b), and (19) into Eq. (18), performing the integration over $|\mathbf{q}'|$, and by subsequently removing the integrals over $\hat{\mathbf{\Omega}}$, together with exponents $\exp(iK_r\hat{\mathbf{\Omega}}\cdot\mathbf{r}_d)$ which are common for all terms. We write the final result as

$$I(\mathbf{r},\hat{\mathbf{\Omega}},t,\tau) = I_0(\mathbf{r},\hat{\mathbf{\Omega}},t,\tau) + \int \mu_s p(\hat{\mathbf{\Omega}},\hat{\mathbf{\Omega}}') \times\exp(-\mu_t|\mathbf{r}-\mathbf{r}_s|)I(\mathbf{r}_s,\hat{\mathbf{\Omega}}',t,\tau) \times\Phi(\mathbf{r},\mathbf{r}_s,\hat{\mathbf{\Omega}},\hat{\mathbf{\Omega}}',t,\tau)d|\mathbf{r}-\mathbf{r}_s|d\Omega', \tag{22}$$

where it is assumed that $\mathbf{r}_{cs}\approx\mathbf{r}_s$, and we also removed now redundant subscript c from the center-of-gravity coordinate $\mathbf{r}_c$. Equation (22) is similar to the previously derived correlation transfer equations for moving scatterers [34,37]. The time-varying specific intensity $I(\mathbf{r},\hat{\mathbf{\Omega}},t,\tau)$ is given as a sum of the unscattered term $I_0(\mathbf{r},\hat{\mathbf{\Omega}},t,\tau)$ and all time-varying specific intensities scattered into direction $\hat{\mathbf{\Omega}}$. The factor $\Phi(\mathbf{r},\mathbf{r}_s,\hat{\mathbf{\Omega}},\hat{\mathbf{\Omega}}',t,\tau)=\exp[i\Psi_d(\mathbf{r}_s,\hat{\mathbf{\Omega}},\hat{\mathbf{\Omega}}',t,\tau)] \times\exp[i\Psi_n(\mathbf{r},\mathbf{r}_s,t,\tau)]$ accounts for the ultrasound-induced optical phase increments due to both mechanisms of modulation. The factor $\Psi_d(\mathbf{r}_s,\hat{\mathbf{\Omega}},\hat{\mathbf{\Omega}}',t,\tau)=-K_r(\hat{\mathbf{\Omega}}-\hat{\mathbf{\Omega}}')\cdot\Delta\mathbf{e}(\mathbf{r}_s,t,\tau)$ that is due to the ultrasound-induced displacement of the optical scatterers is given by

$$\Psi_d(\mathbf{r}_s,\hat{\mathbf{\Omega}},\hat{\mathbf{\Omega}}',t,\tau) = \Lambda_d[(\hat{\mathbf{\Omega}}-\hat{\mathbf{\Omega}}')\cdot\hat{\mathbf{\Omega}}_a]\sin\left(\omega_a\frac{\tau}{2}\right) \times\cos\left[\omega_a\left(t+\frac{\tau}{2}\right)-\mathbf{k}_a\cdot\mathbf{r}_s-\phi_a+\phi\right], \tag{23}$$

where $\Lambda_d=2K_rS_aP_0/(k_a\rho v_a^2)$.

The differential form of the CTE is obtained by taking the gradient of the integral form of the CTE [Eq. (22)] in the $\hat{\mathbf{\Omega}}$ direction [29]. By applying $\hat{\mathbf{\Omega}}\cdot\partial/\partial\mathbf{r}$ to Eq. (22), we have

$$\hat{\mathbf{\Omega}}\frac{\partial I(\mathbf{r},\hat{\mathbf{\Omega}},t,\tau)}{\partial\mathbf{r}} = \hat{\mathbf{\Omega}}\frac{\partial I_0(\mathbf{r},\hat{\mathbf{\Omega}},t,\tau)}{\partial\mathbf{r}} + \int_{4\pi}\mu_s p(\hat{\mathbf{\Omega}},\hat{\mathbf{\Omega}}')\left(\hat{\mathbf{\Omega}}\frac{\partial}{\partial\mathbf{r}}\int_{\mathbf{r}_0}^{\mathbf{r}}\Phi(\mathbf{r},\mathbf{r}_s,\hat{\mathbf{\Omega}},\hat{\mathbf{\Omega}}',t,\tau)\exp(-\mu_t|\mathbf{r}-\mathbf{r}_s|)I(\mathbf{r}_s,\hat{\mathbf{\Omega}}',t,\tau)d|\mathbf{r}-\mathbf{r}_s|\right)d\Omega'. \tag{24}$$

We denote with $D_{\{\}}$ the derivative in the wavy brackets on the right-hand side of Eq. (24) and express its value as

$$D_{\{\}} = \Phi(\mathbf{r},\mathbf{r},\hat{\mathbf{\Omega}},\hat{\mathbf{\Omega}}',t,\tau)I(\mathbf{r},\hat{\mathbf{\Omega}}',t,\tau) - \int_{\mathbf{r}_0}^{\mathbf{r}}\mu_t\Phi(\mathbf{r},\mathbf{r}_s,\hat{\mathbf{\Omega}},\hat{\mathbf{\Omega}}',t,\tau)\exp(-\mu_t|\mathbf{r}-\mathbf{r}_s|)I(\mathbf{r}_s,\hat{\mathbf{\Omega}}',t,\tau)d|\mathbf{r}-\mathbf{r}_s| + \int_{\mathbf{r}_0}^{\mathbf{r}}\hat{\mathbf{\Omega}}\frac{\partial\Phi(\mathbf{r},\mathbf{r}_s,\hat{\mathbf{\Omega}},\hat{\mathbf{\Omega}}',t,\tau)}{\partial\mathbf{r}}\exp(-\mu_t|\mathbf{r}-\mathbf{r}_s|)I(\mathbf{r}_s,\hat{\mathbf{\Omega}}',t,\tau)d|\mathbf{r}-\mathbf{r}_s|. \tag{25}$$

Next, we substitute the expressions from Eqs. (25) and (22) into Eq. (24) to obtain

$$\left(\hat{\mathbf{\Omega}}\frac{\partial}{\partial\mathbf{r}}+\mu_t\right)I(\mathbf{r},\hat{\mathbf{\Omega}},t,\tau) = \left(\hat{\mathbf{\Omega}}\frac{\partial}{\partial\mathbf{r}}+\mu_t\right)I_0(\mathbf{r},\hat{\mathbf{\Omega}},t,\tau) + \mu_s\int_{4\pi}p(\hat{\mathbf{\Omega}},\hat{\mathbf{\Omega}}')\exp[i\Psi_d(\mathbf{r},\hat{\mathbf{\Omega}},\hat{\mathbf{\Omega}}',t,\tau)]I(\mathbf{r},\hat{\mathbf{\Omega}}',t,\tau)d\Omega' + \tilde{\Lambda}_n(\mathbf{r},t,\tau)\mu_s\int_{4\pi}p(\hat{\mathbf{\Omega}},\hat{\mathbf{\Omega}}')\int_{\mathbf{r}_0}^{\mathbf{r}}\Phi(\mathbf{r},\mathbf{r}_s,\hat{\mathbf{\Omega}},\hat{\mathbf{\Omega}}',t,\tau)\exp(-\mu_t|\mathbf{r}-\mathbf{r}_s|)I(\mathbf{r}_s,\hat{\mathbf{\Omega}}',t,\tau)d|\mathbf{r}-\mathbf{r}_s|d\Omega', \tag{26}$$

where $\hat{\mathbf{\Omega}}\cdot\partial\Phi(\mathbf{r},\mathbf{r}_s,\hat{\mathbf{\Omega}},\hat{\mathbf{\Omega}}',t,\tau)/\partial\mathbf{r}$ is represented as $\tilde{\Lambda}_n(\mathbf{r},t,\tau)\Phi(\mathbf{r},\mathbf{r}_s,\hat{\mathbf{\Omega}},\hat{\mathbf{\Omega}}',t,\tau)$, and

$$\tilde{\Lambda}_n(\mathbf{r},t,\tau)=ik_a\Lambda_n\sin\left(\omega_a\frac{\tau}{2}\right)\sin\left[\omega_a\left(t+\frac{\tau}{2}\right)-\mathbf{k}_a\cdot\mathbf{r}+\phi\right]. \tag{27}$$

After substitution of Eq. (22) into Eq. (26), we obtain the final expression for the differential form of the CTE,

$$\left(\hat{\mathbf{\Omega}}\frac{\partial}{\partial\mathbf{r}}+\mu_t-\tilde{\Lambda}_n(\mathbf{r},t,\tau)\right)I(\mathbf{r},\hat{\mathbf{\Omega}},t,\tau)$$
$$=\mu_s\int_{4\pi}p(\hat{\mathbf{\Omega}},\hat{\mathbf{\Omega}}')\exp[i\Psi_d(\mathbf{r},\hat{\mathbf{\Omega}},\hat{\mathbf{\Omega}}',t,\tau)]I(\mathbf{r},\hat{\mathbf{\Omega}}',t,\tau)d\Omega', \tag{28}$$

where $(\hat{\mathbf{\Omega}}\cdot\partial/\partial\mathbf{r}+\mu_t-\tilde{\Lambda}_n(\mathbf{r},t,\tau))\ I_0(\mathbf{r},\hat{\mathbf{\Omega}},t,\tau)\approx 0$ in the region where the Green's function given by Eq. (2) is valid. Also, after several extinction lengths from the source, the coherent time-varying specific intensity becomes negligible in respect to $I(\mathbf{r},\hat{\mathbf{\Omega}},t,\tau)$.

Compared to the CTE where the optical scatterers are undergoing Brownian motion [29,37], in Eq. (28) we have a similar factor $\Psi_d(\ )$ that is due to the ultrasound-induced movement of the optical scatterers, and a new term $\tilde{\Lambda}_n(\ )$.

The time-varying specific intensity $I(\mathbf{r},\hat{\mathbf{\Omega}},t,\tau)$ in the case of ultrasound modulation depends on both time t and time increment τ. Of most practical interest is to find the power spectral density of the ultrasound-modulated light, which implies the availability of an analytical solution for $I(\mathbf{r},\hat{\mathbf{\Omega}},\tau)$. Unfortunately, due to correlations among the ultrasound-induced optical phase increments, it is difficult to create a simple equation for $I(\mathbf{r},\hat{\mathbf{\Omega}},\tau)$ based on Eqs. (28) and (21). In this paper we present a Monte Carlo algorithm which can be used to simulate various configurations for ultrasonic modulation of light in optically scattering samples. It should also be possible to adapt the numerical codes developed for the Boltzmann equation to calculate the power spectral density of the ultrasound-modulated light based on Eq. (28). Also, in the diffusion regime, and for ultrasound wavelengths which satisfy $k_a l_{tr}\gg 1$, it is possible to significantly simplify the expression for $I(\mathbf{r},\hat{\mathbf{\Omega}},\tau)$ by preaveraging [37] the ultrasound-induced optical phase increments in Eq. (22). A formal derivation of the CTE for ultrasound-modulated light was presented in Ref. [42].

IV. MONTE CARLO SIMULATION

We developed a Monte Carlo (MC) algorithm which can, based on Eq. (22), calculate the power spectrum of ultrasound-modulated light when a focused ultrasound field is present in an optically scattering medium with a heterogeneous distribution of optical parameters. The optically scattering medium is divided along the Cartesian axes into cells, which are enumerated by vectors $\mathbf{n}$ with integer coordinates $\{n_x,n_y,n_z\}$ assigned to each cell. We also assign an individual value of the optical absorption and the scattering coefficient to each cell, as well as the scattering anisotropy factor (average cosine of the scattering angle), where a Henyey-Greenstein scattering phase function is assumed [43]. We further assign to each cell an average ultrasound propagation direction $\hat{\mathbf{\Omega}}_{a,\mathbf{n}}$, pressure amplitude $P_{0,\mathbf{n}}$, and phase $\phi_{\mathbf{n}}$, assuming that the dimensions of the cell are much smaller than the ultrasound wavelength so that within each cell, the ultrasound field can be approximated with $P_{\mathbf{n}}(t)=P_{0,\mathbf{n}}\cos(\omega_a t+\phi_{\mathbf{n}})$. The procedure for propagation of the photon packets in the MC is analogous to the previously described algorithms [25,44], with the only difference being that at each crossing of the cell boundaries, the remaining length of the photon free path is adjusted in accordance with the extinction coefficient within the cell that the photon packet is entering. This simulation approach should be sufficiently accurate for calculation of the power spectral density in thick scattering samples, when the light is completely diffused. In other cases, more rigorous approach could be used, which takes into account contributions from all the scattering orders [45,46]. The trajectory of each photon consists of many small steps, which are determined by all of the scattering events and cell boundaries along the way. For each small photon step of length l_i within cell $\mathbf{m}$, the optical phase increment that is due to ultrasound-induced index of refraction changes is calculated as $\Delta\varphi_{n,i}=k_0 n_0 l_i P_{\mathbf{m}}(t)\,\eta/(\rho v_a^2)$, and we express it as

$$\Delta\varphi_{n,i}=P_{n,\cos,i}\cos(\omega_a t)+P_{n,\sin,i}\sin(\omega_a t). \tag{29}$$

The factors $P_{n,\cos,i}$ and $P_{n,\sin,i}$ in Eq. (29) are calculated as $k_0 n_0 l_i\eta(\rho v_a^2)^{-1}P_{0,\mathbf{m}}\cos(\phi_{\mathbf{m}})$, and $-k_0 n_0 l_i\eta(\rho v_a^2)^{-1}P_{0,\mathbf{m}}\times\sin(\phi_{\mathbf{m}})$, respectively.

Similarly, for each scattering event j within cell $\mathbf{n}$, the optical phase increment due to ultrasound-induced scatterer displacement is calculated as $\Delta\varphi_{d,j}=k_0 n_0(k_a\rho v_a^2)^{-1}\hat{\Omega}_{a,\mathbf{n}}\cdot(\hat{\mathbf{\Omega}}_{\mathrm{inc}}-\hat{\mathbf{\Omega}}_{\mathrm{sc}})P_{0,\mathbf{n}}\sin(\omega_a t+\phi_{\mathbf{n}})$, and we express it as

$$\Delta\varphi_{d,j}=P_{d,\cos,j}\cos(\omega_a t)+P_{d,\sin,j}\sin(\omega_a t). \tag{30}$$

In Eq. (30), we use $P_{d,\cos,j}=k_0 n_0(k_a\rho v_a^2)^{-1}\hat{\mathbf{\Omega}}_{a,\mathbf{n}}\cdot(\hat{\mathbf{\Omega}}_{\mathrm{inc}}-\hat{\mathbf{\Omega}}_{\mathrm{sc}})\times P_{0,\mathbf{n}}\sin(\phi_{\mathbf{n}})$, $P_{d,\sin,j}=k_0 n_0(k_a\rho v_a^2)^{-1}\hat{\mathbf{\Omega}}_{a,\mathbf{n}}\cdot(\hat{\mathbf{\Omega}}_{\mathrm{inc}}-\hat{\mathbf{\Omega}}_{\mathrm{sc}})P_{0,\mathbf{n}}\times\cos(\phi_{\mathbf{n}})$. $\hat{\mathbf{\Omega}}_{\mathrm{inc}}$ and $\hat{\mathbf{\Omega}}_{\mathrm{sc}}$ are incident and scattered photon directions, respectively, and we assume for simplicity that the optical scatterers are following the ultrasound-induced movement of the surrounding medium in both amplitude and phase.

At each scattering event, the total ultrasound-induced phase of the photon packet accumulated up to this point is $\Delta\varphi=A\cos(\omega_a t+\phi)$, where $A\cos(\phi)=\Sigma_i P_{n,\cos,i}+\Sigma_j P_{d,\cos,j}$, $A\sin(\phi)=-\Sigma_i P_{n,\sin,i}-\Sigma_j P_{d,\sin,j}$, and i and j count all of the previous steps and scattering events of the photon packet. The expression for the temporal autocorrelation of the photon packet is given by

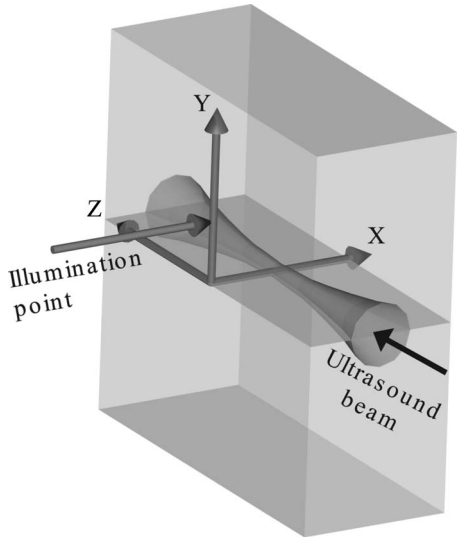

FIG. 2. Configuration for ultrasonic modulation of light in an optically scattering slab.

$$G(t,\tau) = \exp(iA\{\cos(\omega_a t + \phi) - \cos[\omega_a(t+\tau) + \phi]\}). \tag{31}$$

We use $\exp[iA\cos(\phi)] = \Sigma_{m=-\infty}^{+\infty} i^m J_m(A)\exp(im\phi)$ to further develop Eq. (31), where $J_m(A)$ is the Bessel function of the first kind of order m. We arrive then at the expression

$$\frac{\omega_a}{2\pi}\int_0^{2\pi/\omega_a} G(t,\tau)dt = J_0^2(A) + \sum_{m=1}^{+\infty} 2J_m^2(A)\cos(m\omega_a\tau). \tag{32}$$

In the simulation, quantity A is calculated at each scattering event, and the values of $\Delta M_0(\mathbf{n}) = J_0^2(A)\Delta W$ and $\Delta M_1(\mathbf{n}) = 2J_1^2(A)\Delta W$ are obtained, where $\Delta W = W\mu_{a,\mathbf{n}}/\mu_{t,\mathbf{n}}$, and W is the current weight of a photon packet at the scattering event which happened in cell $\mathbf{n}$. At the end of the simulation of all of the photon packets, sums $M_0(\mathbf{n}) = \Sigma\Delta M_0(\mathbf{n})/\mu_{a,\mathbf{n}}$ and $M_1(\mathbf{n}) = \Sigma\Delta M_1(\mathbf{n})/\mu_{a,\mathbf{n}}$ of the increments for all of the scattering events that happened in cell $\mathbf{n}$ are proportional to the amplitudes of the zero and the first harmonics, respectively, of the power spectrum of the ultrasound-modulated light.

The sample in our simulation is an optically scattering slab infinitely wide in the Y and Z directions, with a thickness of $L=20$ mm along the X axis (Fig. 2). We use $\mu_a = 0.1$ cm^{-1} and $\mu_s = 10$ cm^{-1} in the entire slab, which are representative of soft biological tissue for visible and near-infrared light, and, for simplicity, assume isotropic scattering. A focused ultrasound beam with a monochromatic frequency of 1 MHz, focal length of 40 mm, and aperture diameter of 25.4 mm is positioned parallel to the Z axis within the slab and spaced at equal distances from the slab surfaces. The focal spot of the transducer is at $\{x,y,z\} = \{10\text{ mm}, 0\text{ mm}, 0\text{ mm}\}$, and the pressure amplitude at the focus is $P_0 = 10^5$ Pa. A pencil light source with a wavelength of 532 nm irradiates the scattering slab from the $x<0$ half-space, at position $\{x,y,z\} = \{0\text{ mm}, 10\text{ mm}, 0\text{ mm}\}$. We assume the same optical index of refraction $n_0 = 1.33$ in whole space, a mass density of the medium $\rho = 10^3$ kg m^{-3}, an ultrasound velocity $v_a = 1480$ ms^{-1}, and an elasto-optical coefficient of water at room temperature $\eta = 0.32$. The distributions of the ultrasound pressure and phase are calculated with publicly available software Field II [47], and the ultrasound propagation directions are subsequently obtained by taking the gradient of the ultrasound phase. The cell grid is centered around the focal spot of the transducer, and it is 10 cm wide in both the Y and Z directions in order to minimize the error of the simulation within the central region. The dimensions of the cells are $\Delta x = 0.5$ mm, $\Delta y = 0.5$ mm, and $\Delta z = 0.1$ mm, such that the change in the ultrasound phase within the cell is small.

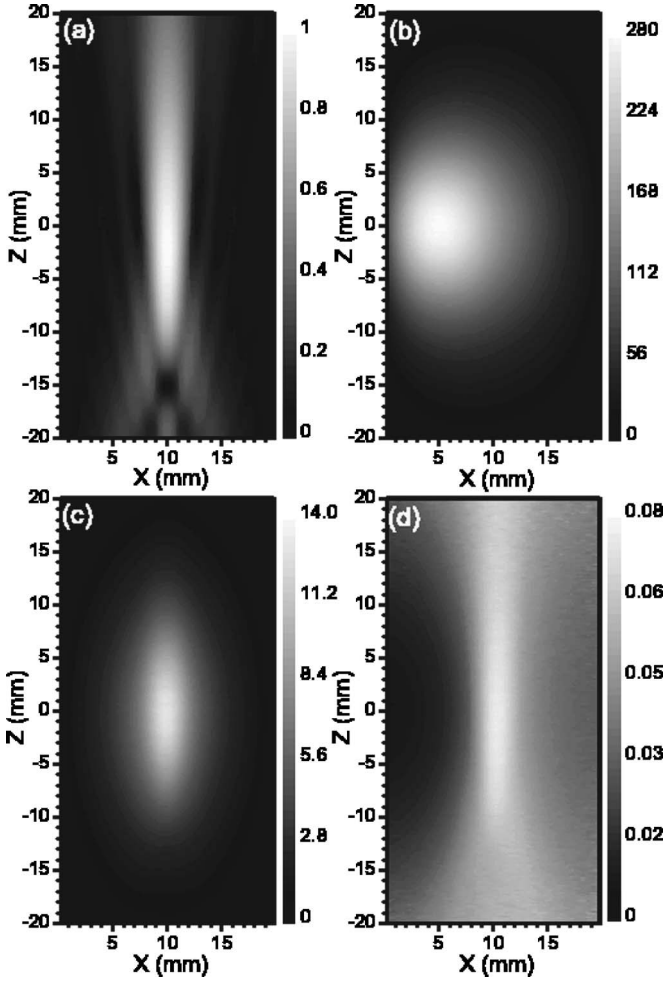

FIG. 3. Monte Carlo simulation results for an optically scattering slab in a plane defined by $y=0$ mm, which contains the axis of the ultrasound beam. (a) Distribution of the ultrasound pressure in 10^5 Pa. (b) Distribution of the amplitude of the zero harmonic $[M_0(\mathbf{n})]$ of the power spectrum of ultrasound-modulated light in arbitrary units. (c) Distribution of the amplitude of the first harmonic $[M_1(\mathbf{n})]$ of the power spectrum of ultrasound-modulated light in arbitrary units. (d) Distribution of the modulation depth calculated as $M_1(\mathbf{n})/M_0(\mathbf{n})$.

Figure 3(a) presents the ultrasound pressure distribution within the slab in plane $y=0$ mm, which contains the axis of the ultrasound beam. In Figs. 3(b) and 3(c), we plot the am-

plitudes of the zero $[M_0(\mathbf{n})]$ and the first $[M_1(\mathbf{n})]$ harmonics of the power spectrum of the ultrasound-modulated light in the same plane ($y=0$ mm). Since the light source is at $y=10$ mm, the maximum of the distribution $M_0(\mathbf{n})$ in plane $y=0$ mm is not at the point of light incidence ($x=0$ mm). Figure 3(c) shows that the distribution $M_1(\mathbf{n})$ follows the profile of the ultrasound focal zone, which confirms the assumption that we used to explain UOT experimental results. Finally, in Fig. 3(d) we plot the modulation depth in the $y=0$ mm plane, calculated as $M_1(\mathbf{n})/M_0(\mathbf{n})$. The modulation depth peaks at 8% at the ultrasound focus. The value of the modulation depth is significantly lower at places closer to the point of light incidence, due to the very high intensity of the unmodulated light. On both sides of the slab, the modulation depth in the $y=0$ mm plane increases at points more distant from the light source, due to the increased probability of the light interacting with the ultrasound along the way. However, the total amount of available light at these points is low. In finding the optimal position for the highest signal-to-noise ratio of the measurement, we should consider both the modulation depth and the total available optical intensity.

V. CONCLUSION

In conclusion, based on the ladder approximation of the Bethe-Salpeter equation, we have developed integral and differential forms of the CTE for ultrasound-modulated light in optically turbid media. We have also developed a Monte Carlo algorithm which can be used to calculate the power spectrum of the ultrasound-modulated light in optically turbid media, with heterogeneous distributions of optical parameters and focused ultrasound fields. The derivations are valid within the weak-scattering approximation, the medical ultrasound frequency range and moderate ultrasound pressures. We expect that the CTE will help to better model UOT experiments for estimations of sensitivity, resolution, and signal-to-noise ratios. Further development of the theory is necessary to address tightly focused ultrasound fields with very high ultrasound pressures.

APPENDIX: DERIVATION OF THE MEAN GREEN'S FUNCTION

To solve the Dyson equation [Eq. (6)], we first assume that the mean Green's function $G_s(\mathbf{r}_b,\mathbf{r}_a,t)$ from $\mathbf{r}_a$ to $\mathbf{r}_b$ can be represented as

$$G_s(\mathbf{r}_b,\mathbf{r}_a,t)=G_a(\mathbf{r}_b,\mathbf{r}_a,t)\chi(\mathbf{r}_b,\mathbf{r}_a,t). \tag{A1}$$

By substituting Eq. (A1) into Eq. (6), we obtain

$$G_a(\mathbf{r}_b,\mathbf{r}_a,t)\chi(\mathbf{r}_b,\mathbf{r}_a,t)=G_a(\mathbf{r}_b,\mathbf{r}_a,t)-\int\frac{f(\hat{\mathbf{\Omega}}_{sb},\hat{\mathbf{\Omega}}_{as})\chi(\mathbf{r}_b,\mathbf{r}_s,t)}{4\pi|\mathbf{r}_b-\mathbf{r}_s||\mathbf{r}_s-\mathbf{r}_a|}\times\exp[ik_0n_0F(\mathbf{r}_s)]\rho_s d\mathbf{r}_s, \tag{A2}$$

where

$$F(\mathbf{r}_s)=|\mathbf{r}_a-\mathbf{r}_s|[1+\xi(\mathbf{r}_s,\mathbf{r}_a,t)]+|\mathbf{r}_s-\mathbf{r}_b|[1+\xi(\mathbf{r}_b,\mathbf{r}_s,t)]+\mathbf{e}_s(t)\cdot(\hat{\mathbf{\Omega}}_{as}-\hat{\mathbf{\Omega}}_{sb}). \tag{A3}$$

Without loss of generality, we assume that the ultrasound propagates along the Z axis. In order to simplify the appearance of further expressions, the following notation will be used: the distance between two points at $\mathbf{r}_a$ with coordinates $\{x_a,y_a,z_a\}$ and $\mathbf{r}_b$ with coordinates $\{x_b,y_b,z_b\}$ will be written as r_{ab}, where $r_{ab}\equiv|\mathbf{r}_a-\mathbf{r}_b|$; we will denote with $\{x_{ab},y_{ab},z_{ab}\}$ coordinates of the vector difference $\mathbf{r}_a-\mathbf{r}_b$; the functions $\xi(\mathbf{r}_a,\mathbf{r}_b,t)$ and $\chi(\mathbf{r}_b,\mathbf{r}_a,t)$ will be written as ξ_{ab} and χ_{ba}, respectively; partial derivatives will be written using the appropriate subscripts [for example, $F_x(\mathbf{r}_s)\equiv\partial F(\mathbf{r}_s)/\partial x_s$, $F_{xy}(\mathbf{r}_s)\equiv\partial^2F(\mathbf{r}_s)/\partial x_s\partial y_s$].

We first resolve the following integral:

$$I_{xy}=-\int\int\frac{f(\hat{\mathbf{\Omega}}_{sb},\hat{\mathbf{\Omega}}_{as})\chi_{bs}}{4\pi r_{as}r_{sb}}\exp[ik_0n_0F(\mathbf{r}_s)]\rho_s dx_s dy_s \tag{A4}$$

in the X-Y plane from Eq. (A2). The factor $k_0n_0F(\mathbf{r}_s)$ in Eq. (A4) changes much faster than the slow varying part $\rho_s f(\hat{\mathbf{\Omega}}_{sb},\hat{\mathbf{\Omega}}_{as})\chi_{bs}/(4\pi r_{as}r_{sb})$, so we obtain the approximate value of I_{xy} by using the method of stationary phase. The integral in n-dimensional space ($x\in R^n$) of the form

$$I(\lambda)=\int_D g(x)\exp[i\lambda f(x)]dx, \tag{A5}$$

where the phase $\lambda f(x)$ oscillates much faster than function $g(x)$, can be approximated as

$$I(\lambda)\approx\frac{g(x_0)}{\sqrt{|D(A)|}}\exp\left(i\lambda f(x_0)+i\pi\frac{\sigma}{4}\right)\left(\frac{2\pi}{\lambda}\right)^{n/2}. \tag{A6}$$

In Eq. (A6), x_0 is the single minimum of $f(x)$; A is the Hessian of $f(x)$ given by $A=[\ \partial^2f(x)/\partial x_i\partial x_j|_{x=x_0}]$; σ is the signature of A calculated as the difference between the number of positive and negative eigenvalues of A; and condition $D(A)\neq0$ is satisfied, where $D(A)$ is the determinant of A. If there is more than one minimum of $f(x)$, then summation over all minima should be performed.

The functions ξ_{as} and ξ_{sb}, as well as the term $\mathbf{e}_s(t)\cdot(\hat{\mathbf{\Omega}}_{as}-\hat{\mathbf{\Omega}}_{sb})$, are independent from x_s and y_s, and the partial derivatives of $F(\mathbf{r}_s)$ can be calculated as

$$F_x(\mathbf{r}_s)=x_{sa}(1+\xi_{as})/r_{as}+x_{sb}(1+\xi_{sb})/r_{sb},$$

$$F_y(\mathbf{r}_s)=y_{sa}(1+\xi_{as})/r_{as}+y_{sb}(1+\xi_{sb})/r_{sb}. \tag{A7}$$

The extrema of $F(\mathbf{r}_s)$ are given by $F_x(\mathbf{r}_s)=0$ and $F_y(\mathbf{r}_s)=0$, so we obtain the following relations:

$$x_{sa}/x_{sb}=-r_{as}(1+\xi_{sb})/[r_{sb}(1+\xi_{as})],$$

$$y_{sa}/y_{sb}=-r_{as}(1+\xi_{sb})/[r_{sb}(1+\xi_{as})]. \tag{A8}$$

Since we consider only small ultrasound-induced optical phase perturbations ($|\xi_{sb}|<1$, $|\xi_{as}|<1$), from Eq. (A8) we have $x_{sa}/x_{sb}\leqslant0$ and $y_{sa}/y_{sb}\leqslant0$.

The second partial derivatives of $F(\mathbf{r}_s)$ are

$$F_{xx}(\mathbf{r}_s) = \frac{(y_{as}^2 + z_{as}^2)(1+\xi_{as})}{r_{as}^3} + \frac{(y_{sb}^2 + z_{sb}^2)(1+\xi_{sb})}{r_{sb}^3},$$

$$F_{yy}(\mathbf{r}_s) = \frac{(x_{as}^2 + z_{as}^2)(1+\xi_{as})}{r_{as}^3} + \frac{(x_{sb}^2 + z_{sb}^2)(1+\xi_{sb})}{r_{sb}^3},$$

$$F_{xy}(\mathbf{r}_s) = -\frac{x_{sa}y_{sa}(1+\xi_{as})}{r_{as}^3} - \frac{x_{sb}y_{sb}(1+\xi_{sb})}{r_{sb}^3}, \tag{A9}$$

and we can calculate $D(A)$ with the help of Eq. (A8) as

$$D(A) = z_{as}^2(1+\xi_{as})^2/r_{as}^4 + z_{sb}^2(1+\xi_{sb})^2/r_{sb}^4 + (1+\xi_{as})(1+\xi_{sb}) \times (z_{sb}^2 r_{as}^2 + z_{as}^2 r_{sb}^2)/(r_{as}r_{sb})^3. \tag{A10}$$

Based on Eqs. (A9) and (A10), A is positive definite [$D(A)>0$ and also $F_{xx}(\mathbf{r}_s)+F_{yy}(\mathbf{r}_s)>0$] and $\sigma=2$. For any given z_s, we denote with $\{x_s, y_s, z_s\}$ the coordinates of a single minimum point $\mathbf{r}_s$ of $F(\mathbf{r})$. We now apply the approximation from Eq. (A6) to the integral in Eq. (A4) and obtain

$$I_{xy} = -\frac{i\rho_s}{2k_0 n_0} \frac{f(\hat{\mathbf{\Omega}}_{as}, \hat{\mathbf{\Omega}}_{sb})\chi_{bs}}{r_{as}r_{sb}\sqrt{D(A)}} \exp[\mathbf{e}_s(t)\cdot(\hat{\mathbf{\Omega}}_{as} - \hat{\mathbf{\Omega}}_{sb})] \times \exp\{ik_0 n_0[r_{as}(1+\xi_{as}) + r_{sb}(1+\xi_{sb})]\}, \tag{A11}$$

where x_s and y_s are obtained by solving Eq. (A8). We consider ξ_{sb} and ξ_{as} to be small perturbations of $F(\mathbf{r}_s)$, and we assume that we make only a small error by using the solution of unperturbed $F(\mathbf{r}_s)$ for x_s and y_s. From Eq. (A8) when $\xi_{sb}=0$ and $\xi_{as}=0$, we have $x_{sa}/x_{sb}=-r_{as}/r_{sb}$, $y_{sa}/y_{sb}=-r_{as}/r_{sb}$, and $z_{sa}/z_{sb}=-\gamma r_{as}/r_{sb}$, where $\gamma=1$ if z_s belongs to the interval bounded by z_a and z_b, and $\gamma=-1$ for all other values of z_s. We further obtain the relations

$$x_s = \frac{x_a z_{sb} - x_b \gamma z_{sa}}{z_{sb} - \gamma z_{sa}}, \quad y_s = \frac{y_a z_{sb} - y_b \gamma z_{sa}}{z_{sb} - \gamma z_{sa}},$$

$$x_{sa} = \frac{\gamma x_{ab} z_{sa}}{z_{sb} - \gamma z_{sa}}, \quad y_{sa} = \frac{\gamma y_{ab} z_{sa}}{z_{sb} - \gamma z_{sa}},$$

$$x_{sb} = \frac{x_{ab} z_{sb}}{z_{sb} - \gamma z_{sa}}, \quad y_{sb} = \frac{y_{ab} z_{sb}}{z_{sb} - \gamma z_{sa}},$$

$$r_{as} = \frac{|z_{sa}|}{z_{asb}} r_{abs}, \quad r_{sb} = \frac{|z_{sb}|}{z_{asb}} r_{abs}, \tag{A12}$$

where $z_{asb}=|z_{as}|+|z_{sb}|$, and $r_{asb}=\sqrt{x_{ab}^2+y_{ab}^2+z_{asb}^2}$.

By using the expressions from Eq. (A12), we further obtain $r_{as}r_{sb}\sqrt{D(A)} \approx z_{asb}$, and also

$$\exp\{ik_0 n_0[r_{as}(1+\xi_{as}) + r_{sb}(1+\xi_{sb})]\} \approx \exp\{ik_0 n_0 r_{abs}[1 + (|z_{sa}|\xi_{as} + |z_{sb}|\xi_{sb})/z_{asb}]\}. \tag{A13}$$

When z_s is inside the interval bounded by z_a and z_b, then $z_{asb}=|z_{ab}|$ and the expression in Eq. (A13) is further simplified as

$$\exp\{ik_0 n_0[r_{as}(1+\xi_{as}) + r_{sb}(1+\xi_{sb})]\} \approx \exp[ik_0 n_0 r_{ab}(1+\xi_{ab})]. \tag{A14}$$

After the substitution of Eq. (A11) with obtained approximations into Eq. (A2) and subsequent division by $G_a(\mathbf{r}_b, \mathbf{r}_a, t)$, we have

$$\chi_{ba} = 1 + \frac{i2\pi\rho_s}{k_0 n_0} \int \frac{f(\hat{\mathbf{\Omega}}_{sb}, \hat{\mathbf{\Omega}}_{as})\chi_{bs}}{(z_{asb}/r_{ab})} \times \exp\{ik_0 n_0[V(z_s) + \mathbf{e}_s(t)\cdot(\hat{\mathbf{\Omega}}_{as} - \hat{\mathbf{\Omega}}_{sb})]\} dz_s, \tag{A15}$$

where

$$V(z_s) = r_{abs}\left(1 + \frac{|z_{as}|}{z_{asb}}\xi_{as} + \frac{|z_{sb}|}{z_{asb}}\xi_{sb}\right) - r_{ab}(1+\xi_{ab}). \tag{A16}$$

Without loss of generality, we assume at this point that $z_b > z_a$. Since the rapidly oscillating factor in the exponent on the right-hand side of Eq. (A15) is exactly zero only when $z_s \in (z_a, z_b)$, we assume that the value of the integral for $z_s \notin (z_a, z_b)$ is negligible. When x_s and y_s satisfy the relations in Eqs. (A12), and $z_s \in (z_a, z_b)$, the vectors $\mathbf{r}_b - \mathbf{r}_s$ and $\mathbf{r}_s - \mathbf{r}_a$ are collinear. Consequently, $f(\hat{\mathbf{\Omega}}_{sb}, \hat{\mathbf{\Omega}}_{as}) = f(\hat{\mathbf{\Omega}}, \hat{\mathbf{\Omega}})$, $\hat{\mathbf{\Omega}}_{as} - \hat{\mathbf{\Omega}}_{sb} = 0$, and Eq. (A15) is

$$\chi_{ba} = 1 + \frac{i2\pi\rho_s f(\hat{\mathbf{\Omega}}, \hat{\mathbf{\Omega}})}{k_0 n_0 (\hat{\mathbf{\Omega}}_{ab}\cdot\hat{\mathbf{\Omega}}_a)} \int_{z_a}^{z_b} \chi_{bs} dz_s, \tag{A17}$$

with solution

$$\chi_{ba} = \exp[i2\pi\rho_s f(\hat{\mathbf{\Omega}}, \hat{\mathbf{\Omega}}) r_{ab}/(k_0 n_0)]. \tag{A18}$$

By substituting Eq. (A18) into Eq. (A1), the mean Green's function is

$$G_s(\mathbf{r}_b, \mathbf{r}_a, t) = \frac{\exp[iK(\mathbf{r}_b, \mathbf{r}_a, t)|\mathbf{r}_b - \mathbf{r}_a|]}{-4\pi|\mathbf{r}_b - \mathbf{r}_a|}, \tag{A19}$$

where $K(\mathbf{r}_b, \mathbf{r}_a, t)$ is equal to $k_0 n_0[1+\xi(\mathbf{r}_b, \mathbf{r}_a, t)] + 2\pi\rho_s f(\hat{\mathbf{\Omega}}, \hat{\mathbf{\Omega}})/(k_0 n_0)$.

[1] A. P. Gibson, J. C. Hebden, and S. R. Arridge, Phys. Med. Biol. **50**, R1 (2005).
[2] F. A. Marks, H. W. Tomlinson, and G. W. Brooksby, in Proc. SPIE **1888**, 500 (1993).
[3] L. V. Wang, S. L. Jacques, and X. Zhao, Opt. Lett. **20**, 629 (1995).
[4] M. Kempe, M. Larionov, D. Zaslavsky, and A. Z. Genack, J. Opt. Soc. Am. A **14**, 1151 (1997).
[5] L. V. Wang and G. Ku, Opt. Lett. **23**, 975 (1998).
[6] S. Leveque, A. C. Boccara, M. Lebec, and H. Saint-Jalmes, Opt. Lett. **24**, 181 (1999).
[7] G. Yao, S.-L. Jiao, and L. V. Wang, Opt. Lett. **25**, 734 (2000).
[8] A. Lev, Z. Kotler, and B. G. Sfez, Opt. Lett. **25**, 378 (2000).
[9] M. Hisaka, T. Sugiura, and S. Kawata, J. Opt. Soc. Am. A **18**, 1531 (2001).
[10] J. Li, G. Ku, and L. V. Wang, Appl. Opt. **41**, 6030 (2002).
[11] A. Lev and B. G. Sfez, Opt. Lett. **28**, 1549 (2003).
[12] M. Gross, P. Goy, and M. Al-Koussa, Opt. Lett. **28**, 2482 (2003).
[13] T. W. Murray, L. Sui, G. Maguluri, R. A. Roy, A. Nieva, F. Blonigen, and C. A. DiMarzio, Opt. Lett. **29**, 2509 (2004).
[14] A. Lev, E. Rubanov, B. Sfez, S. Shany, and A. J. Foldes, Opt. Lett. **30**, 1692 (2005).
[15] S. Sakadzic and L. V. Wang, Opt. Lett. **29**, 2770 (2004).
[16] E. Bossy, L. Sui, T. W. Murray, and R. A. Roy, Opt. Lett. **30**, 744 (2005).
[17] W. Leutz and G. Maret, Physica B **204**, 14 (1995).
[18] G. Maret and P. E. Wolf, Z. Phys. B: Condens. Matter **65**, 409 (1987).
[19] G. D. Mahan, W. E. Engler, J. J. Tiemann, and E. G. Uzgiris, Proc. Natl. Acad. Sci. U.S.A. **95**, 14015 (1998).
[20] L. V. Wang, Phys. Rev. Lett. **87**, 043903 (2001).
[21] D. J. Pine, D. A. Weitz, P. M. Chaikin, and E. Herbolzheimer, Phys. Rev. Lett. **60**, 1134 (1988).
[22] S. Sakadzic and L. V. Wang, Phys. Rev. E **66**, 026603 (2002).
[23] A. Lev and B. Sfez, J. Opt. Soc. Am. A **20**, 2347 (2003).
[24] S. Sakadzic and L. V. Wang, Phys. Rev. E **72**, 036620 (2005).
[25] L. V. Wang, Opt. Lett. **26**, 1191 (2001).
[26] G. Yao and L. Wang, Appl. Opt. **43**, 1320 (2004).
[27] U. Frisch, "Wave propagation in random media," *Probabilistic methods in applied mathematics* (Academic, New York, 1968), Vol. 1, pp. 75–198.
[28] Y. N. Barabanenkov, A. G. Vinogradov, Yu. A. Kravtsov, and V. I. Tatarskii, Radiophys. Quantum Electron. **15**, 1420 (1972).
[29] A. Ishimaru, *Wave Propagation and Scattering in Random Media* (Academic, New York, 1978).
[30] M. C. W. van Rossum and Th. M. Nieuwenhuizen, Rev. Mod. Phys. **71**, 313 (1999).
[31] Yu. A. Kravtsov and L. A. Apresyan, "Radiative transfer: new aspects of the old theory," *Progress in Optics* (Elsevier, Amsterdam, 1996), Vol. 36, pp. 179–244.
[32] S. M. Rytov, Yu. A. Kravtsov, and V. I. Tatarskii, *Principles of Statistical Radiophysics 4: Wave Propagation Through Random Media*, 1st ed. (Springer Verlag, Berlin Heidelberg, 1989).
[33] V. L. Kuzmin and V. P. Romanov, Phys. Usp. **39**, 231 (1996).
[34] A. Ishimaru, Radio Sci. **10**, 45 (1975).
[35] M. J. Stephen, Phys. Rev. B **37**, 1 (1988).
[36] F. C. MacKintosh and S. John, Phys. Rev. B **40**, 2383 (1989).
[37] R. L. Dougherty, B. J. Ackerson, N. M. Reguigui, F. Dorri-Nowkoorani, and U. Nobbmann, J. Quant. Spectrosc. Radiat. Transf. **52**, 713 (1994).
[38] F. J. Blonigen, A. Nieva, C. A. DiMarzio, S. Manneville, L. Sui, G. Maguluri, T. W. Murray, and R. A. Roy, Appl. Opt. **44**, 3735 (2005).
[39] Y. N. Barabanenkov, Sov. Phys. JETP **27**, 954 (1968).
[40] S. M. Rytov, Yu. A. Kravtsov, and V. I. Tatarskii, *Principles of Statistical Radiophysics 3: Elements of Random Fields*, 1st ed. (Springer-Verlag, Berlin, Heidelberg, 1989).
[41] J. W. Goodman, *Statistical Optics* (Wiley, New York, 1985).
[42] S. Sakadzic and L. V. Wang, Phys. Rev. Lett. **96**, 163902 (2006).
[43] L. G. Henyey and J. L. Greenstein, Astrophys. J. **93**, 70 (1941).
[44] L. V. Wang, S. L. Jacques, and L.-Q. Zheng, Comput. Methods Programs Biomed. **47**, 131 (1995).
[45] V. L. Kuzmin, I. V. Meglinski, and D. Yu. Churmakov, Sov. Phys. JETP **101**, 22 (2005).
[46] I. V. Meglinski, V. L. Kuzmin, D. Yu. Churmakov, and D. A. Greenhalgh, Proc. R. Soc. London, Ser. A **461**, 43 (2005).
[47] J. A. Jensen and N. B. Svendsen, IEEE Trans. Ultrason. Ferroelectr. Freq. Control **39**, 262 (1992).